

Alma Mater Studiorum Università di Bologna
Archivio istituzionale della ricerca

Luminescent silicon nanocrystals appended with photoswitchable azobenzene units

This is the final peer-reviewed author's accepted manuscript (postprint) of the following publication:

Published Version:

Villa M., Angeloni S., Bianco A., Gradone A., Morandi V., Ceroni P. (2021). Luminescent silicon nanocrystals appended with photoswitchable azobenzene units. *NANOSCALE*, 13(29), 12460-12465 [10.1039/d1nr02328d].

Availability:

This version is available at: <https://hdl.handle.net/11585/850008> since: 2022-01-31

Published:

DOI: <http://doi.org/10.1039/d1nr02328d>

Terms of use:

Some rights reserved. The terms and conditions for the reuse of this version of the manuscript are specified in the publishing policy. For all terms of use and more information see the publisher's website.

This item was downloaded from IRIS Università di Bologna (<https://cris.unibo.it/>).
When citing, please refer to the published version.

(Article begins on next page)

This is the final peer-reviewed accepted manuscript of:

M. Villa, S. Angeloni, A. Bianco, A. Gradone, V. Morandi, P. Ceroni*

“Luminescent silicon nanocrystals appended with photoswitchable azobenzene units”

Nanoscale 2021, 13, 12460–12465

The final published version is available online at:

<https://doi.org/10.1039/D1NR02328D>

Rights / License:

The terms and conditions for the reuse of this version of the manuscript are specified in the publishing policy. For all terms of use and more information see the publisher's website.

This item was downloaded from IRIS Università di Bologna (<https://cris.unibo.it/>)

When citing, please refer to the published version.

Luminescent silicon nanocrystals appended with photoswitchable azobenzene units

Marco Villa,^a Sara Angeloni,^a Alberto Bianco,^a Alessandro Gradone,^{a,b} Vittorio Morandi,^b Paola Ceroni^{a *}

Confinement of multiple azobenzene chromophores covalently linked at the surface of luminescent silicon nanocrystals preserves the photoswitching behavior and modulates the nanocrystal polarity. Concomitantly, the thermal $Z \rightarrow E$ isomerization is strongly accelerated and the nanocrystal luminescence is reduced by an energy transfer process resulting in photosensitized $E \rightarrow Z$ isomerization.

Introduction

Luminescent silicon nanocrystals (SiNCs) are emerging as viable alternatives to traditional luminescent quantum dots.^{1–4} The advantages of SiNCs include the high natural abundance of silicon, lack of any known biological toxicity of Si nanoparticles^{5,6} and robustness of their surface passivation, which is necessary to prevent nanocrystals' oxidation.^{7,8} Their luminescence can be tuned in the visible up to the near infrared region by varying the nanocrystal size. The most distinctive feature of SiNCs is their bright long-lived (tens-to-hundreds of microseconds) luminescence.^{9–13}

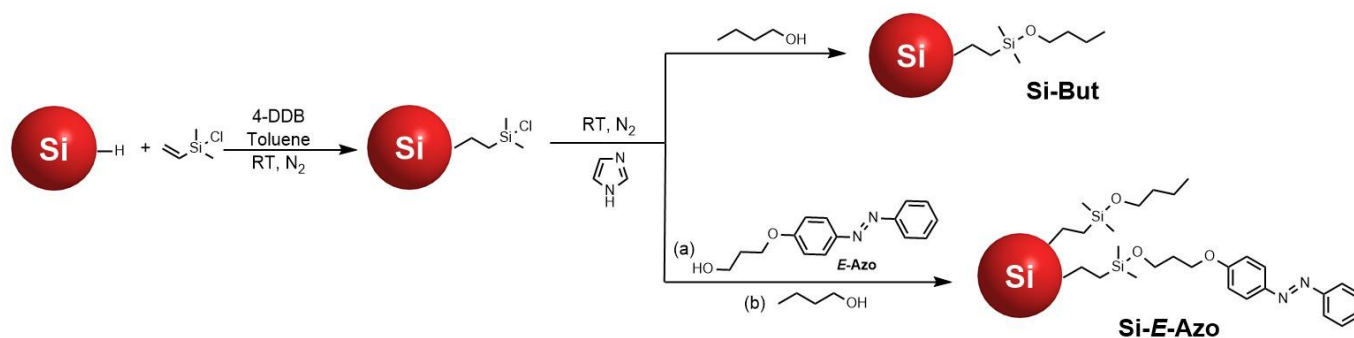
Among molecular photoswitches, azobenzene is one of the most investigated example: it undergoes an efficient and fully reversible photoisomerization reaction. The photoreaction brings about not only a change in colour, but also a large structural rearrangement (the distance between the para carbon atoms of azobenzene decreases from 9.0 to 5.5 Å) and a strong increase in the dipole moment from zero for the planar and symmetric *E* isomer to 3.0 Debye for the *Z* isomer.^{14,15} The increased solubility in polar solvents of the *Z* isomer has been used for controlling self-assembly of surfactants, organogels and foams.^{16–19}

Azobenzene has been thoroughly investigated in conjunction with metallic nanoparticles to induce structural, optical or electronic changes of the resulting hybrid material.^{20–23} Much less is reported about the coupling of azobenzene and luminescent quantum dots. Previous investigations of CdS and CdTe quantum dots functionalised with azobenzene units demonstrated possible modulation of the nanoparticles' luminescent properties by the occurrence of photoinduced electron transfer processes within the hybrid systems.^{24,25}

The covalent coupling of silicon nanocrystals with photoswitching azobenzene units is unprecedented. In the present paper, the interaction of the organic chromophores with the inorganic nanocrystal is studied in terms of the effect of the silicon core on the photochemical and thermal isomerisation of the azobenzene and, *viceversa*, the effect of the azobenzene units on the luminescent properties of the nanocrystals. Furthermore, the different polarity of the *E* and *Z*-isomers allow to disperse the azobenzene-derivatised SiNCs in solvents of different polarity according to the isomerisation state of the peripheral photoswitching units.

Results and discussion

Photoswitchable SiNCs were obtained by a three step procedure (Scheme 1): (i) synthesis of hydride-terminated silicon nanocrystals by thermal disproportionation of hydrogen silsesquioxane (HSQ);^{26,27} (ii) room-temperature hydrosilylation of hydride-terminated SiNCs in the presence of dimethylvinylchlorosilane and 4-decylbenzene diazonium tetrafluoroborate (4-DDB), as radical initiator;^{28,29} (iii) nucleophilic substitution of an alcohol-functionalized azobenzene derivative (**E-Azo**, Scheme 1),³⁰ followed by butanol addition to obtain the co-passivated **Si-E-Azo** sample (Scheme 1). The successive addition of butanol in step (iii) was performed to ensure complete functionalization of chlorosilane derivatives and to achieve a colloiddally stable dispersion of the synthesized nanocrystals.⁵



Scheme 1. Synthetic procedure for the functionalization of hydride-terminated SiNCs by azobenzene chromophore. The reference sample **Si-But** is reported for comparison purposes.

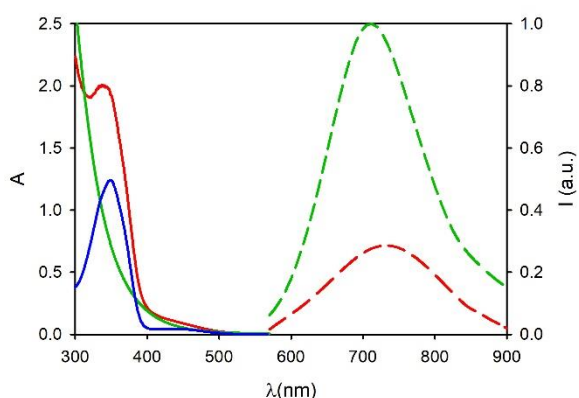


Figure 1. Absorption (solid lines) and photoluminescence spectra (dashed lines) of **Si-But** (3.80×10^{-6} M, green lines) and **Si-E-Azo** (4.00×10^{-6} M, red lines) in toluene. λ_{ex} = 540 nm, where only SiNCs absorb light. For the sake of comparison, the absorption spectrum of **E-Azo** (1.79×10^{-6} M, blue line) is reported.

For the control sample **Si-But**, step (iii) was performed on the same chlorosilane-functionalised SiNC batch upon addition of only butanol (Scheme 1).

The samples were purified, under inert atmosphere, by precipitation, followed by filtration and washing with dry acetonitrile. The resulting SiNCs were dispersed in distilled toluene or cyclohexane under inert atmosphere.

The size distribution of silicon nanocrystals was evaluated by dynamic light scattering (DLS) analysis to evaluate the hydrodynamic volume comprising the organic capping ligands and by scanning transmission electron microscopy (STEM) imaging to estimate the size of only the silicon core. DLS analysis of **Si-E-Azo** (1.00×10^{-6} M) in toluene yields an average hydrodynamic diameter of 10 nm with a low polydispersity index (PDI = 0.13, Figure S3a). A similar hydrodynamic radius (8 nm) is observed for **Si-But** (Figure S3c). STEM analysis shows an average size distribution of the silicon crystalline core of ca. 3 nm ($d = 2.8 \pm 0.4$ nm, Figure S14). As previously demonstrated,³¹ the dimension of the silicon core is determined by the annealing temperature and the successive etching step: SiNCs with a diameter of ca. 3 nm were obtained, in analogy to previously reported samples of alkyl-terminated SiNCs prepared by the same methodology.^{13,32} This result is confirmed also by the luminescence properties (see below).

Photophysical properties. The absorption spectrum of **Si-E-Azo** in toluene exhibits a maximum at 340 nm and a tail up to 550 nm (solid red line, Figure 1). It displays the contribution of both the unstructured absorption tail of the silicon core (see e.g., the reference sample of **Si-But** solid green line, Figure 1) and the typical bands of **E-Azo** chromophore (solid blue line, Figure 1): a very intense π, π^* band in the UV region at 350 nm and a less intense n, π^* band in the visible region at 435 nm. On a quantitative basis, the molar absorption coefficient of **Si-E-Azo** well matches the sum of the molar absorption coefficient of the reference **Si-But** (estimated according to the value reported in ref. 27 for alkyl passivated silicon nanocrystals) and 15 **E-Azo** reference compounds (see SI and Figure S5 for more details). This result demonstrates that each SiNC is functionalized with 15 azobenzene moieties, as an average: this is a very large number of chromophores per nanocrystals, compared to the previously reported SiNCs of comparable size.^{12,13,33}

Table 1. Photophysical properties of **Si-E-Azo** and **Si-Z-Azo**, compared to reference sample **Si-But** at room temperature in toluene solution.

	λ_{em}/nm	Φ_{em}	$\tau/\mu s$
Si-But	710	35%	80
Si-E-Azo	730	10%	45
Si-Z-Azo	730	8%	40

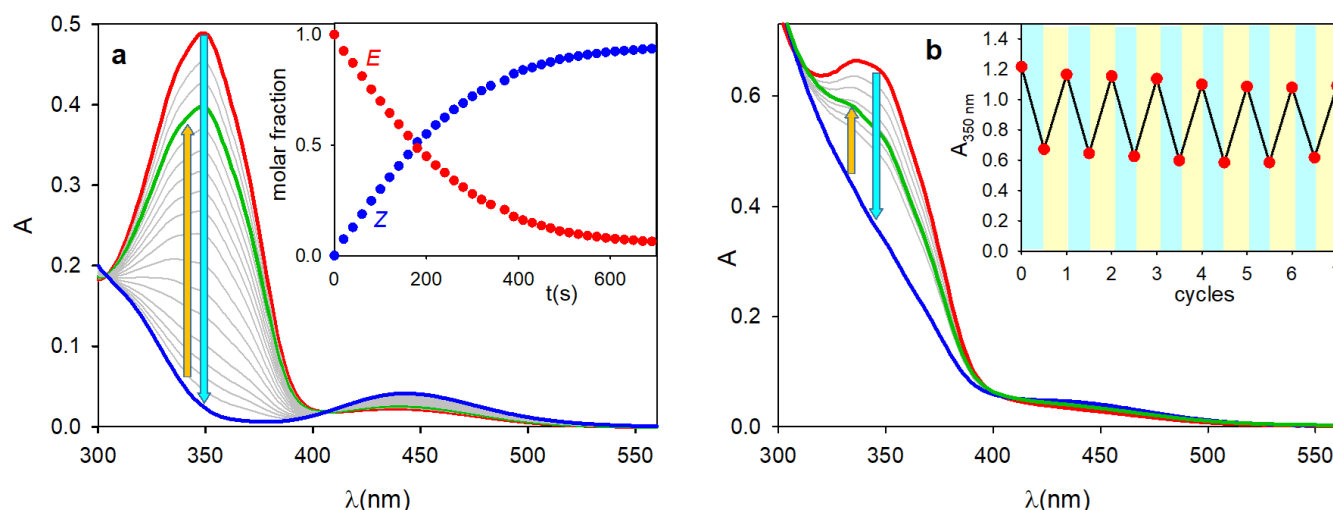


Figure 2. Spectral changes observed upon irradiation of toluene solutions of (a) **E-Azo** (1.77×10^{-5} M) and (b) **Si-E-Azo** (1.00×10^{-6} M) with 365 nm (cyan arrow) and successive irradiation with 436 nm (yellow arrow): red line for *E*-isomer, blue and green lines for the photostationary states obtained upon 365 and 436 nm irradiation, respectively. Inset of panel (a) shows the corresponding change in the molar fractions of the *E* and *Z* isomers during irradiation. Inset of panel (b) shows absorbance changes at 350 nm for the photostationary states obtained for azobenzene-functionalised SiNCs in toluene upon 365-nm (cyan areas) and 436-nm irradiation (yellow areas).

Table 2. Photochemical parameters of **Si-E-Azo** and **Si-Z-Azo** compared to model compounds **E-Azo** and **Z-Azo** at 293 K in degassed toluene solution.

	Photochemical isomerization				Thermal isomerization
	$\lambda_{irr} = 365 \text{ nm}$		$\lambda_{irr} = 436 \text{ nm}$		
	$\Phi_{E \rightarrow Z}$	%E	$\Phi_{Z \rightarrow E}$	%E	$k_{Z \rightarrow E} / s^{-1}$
Azo	15%	<1	34%	72	2.5×10^{-6}
Si-Azo	15%	<1	35%	70	- ^a

^aThe value cannot be estimated since the observed trend does not follow a simple first-order kinetics (see blue circles in Figure 4a).

Upon excitation at 540 nm, where only the silicon core absorbs light, **Si-E-Azo** shows the typical silicon emission band peaked at 730 nm (dashed red line, Figure 1), similar to the **Si-But** sample (dashed green line, Figure 1) and consistent with SiNCs with average core diameter of 3 nm (Figure S4 and Figure S14).^{12,13,34} The lifetime and photoluminescence quantum yield of **Si-E-Azo** is lower than that of the reference **Si-But** (Table 1).

The **Si-Z-Azo** isomer, obtained by photochemical isomerization at 365 nm (blue line in Figure 2b), displays an absorption spectrum compatible with the sum of the Si-core and *Z*-azobenzene units and luminescence properties very similar to the corresponding **Si-E-Azo**.

Photochemical properties. **E-Azo** exhibits the typical photoswitching behavior of azobenzene chromophores (Figure 2a): upon 365 nm irradiation, $E \rightarrow Z$ isomerization occurs with $\Phi_{E \rightarrow Z} = 15\%$ and the corresponding photostationary state (blue line, Figure 2a) is composed by less than 1% of *E* isomer, as estimated by NMR spectroscopy (see inset of Figure 2a and SI for details). Upon irradiation at 436 nm of the so-obtained photostationary state, the reverse $Z \rightarrow E$ isomerization is observed with $\Phi_{Z \rightarrow E} = 34\%$ and a photostationary state (green line, Figure 2a) composed by 72% of *E* isomer (see SI for more details).

Irradiation of **Si-E-Azo** in degassed toluene solution at 365 nm brings about $E \rightarrow Z$ isomerization of the peripheral azobenzene units (Figure 2b) with $\Phi_{E \rightarrow Z} = 15\%$, as estimated by considering the fraction of light absorbed only by the azobenzene chromophores. The corresponding photostationary state (blue line, Figure 2b) is composed by less than 1% of *E* isomer. Indeed, the absorption spectrum of the photostationary state is the sum of the silicon core absorption and 15 **Z-Azo** moieties (Figure S6), based on the molar absorption coefficient of **Z-Azo** previously determined (see SI). No significant change of the hydrodynamic diameter of **Si-Z-Azo** has been observed by DLS analysis (see Figure S3b). Upon irradiation at 436 nm, back $Z \rightarrow E$ isomerization is observed with $\Phi_{Z \rightarrow E} = 35\%$ and a photostationary state (green line, Figure 2b) composed by 70% of *E* isomer.

The photochemical properties of azobenzene units at the surface of SiNCs are similar to those of the model compound (Table 2), demonstrating that there is no significant interaction between the organic chromophores and the inorganic silicon core. This result is expected on the basis of the very short lifetime of the photoreactive singlet excited state of azobenzene.³⁵

It is worth noting that no significant degradation has been observed for the azobenzene functionalized SiNCs in air-equilibrated toluene solution, unless prolonged irradiation is performed in the presence of atmospheric oxygen, likely related to a photo-oxidation of the silicon surface.

On the other hand, in degassed toluene solution, the fatigue resistance is very good (inset of Figure 2b): upon repeated irradiation cycles at 365 nm (cyan area) and 436 nm (yellow



area) of azobenzene-functionalised nanocrystals in toluene, no significant change of the composition of the photostationary states is observed (differently, the air-equilibrated solution deteriorates after only 3 cycles).

Figure 3. Schematic representation of the partition of **Si-E-Azo** and **Si-Z-Azo** isomers between cyclohexane and MeOH.

It is well-known that the azobenzene polarity is substantially different between the *E* and *Z* isomers. A visual demonstration of the different polarity of the **Si-E-Azo** and **Si-Z-Azo** samples is reported in Figure 3: the partition ratio of **Si-E-Azo** between cyclohexane and methanol is 65:35, while that of **Si-Z-Azo** is <20:80. A careful estimation of the partition coefficient of **Si-Z-Azo** is made difficult by the extremely fast thermal isomerization of **Si-Z-Azo** to **Si-E-Azo** (*vide infra*).

Thermal Z→E isomerization. Thermal isomerization of **Z-Azo** with complete recovery of the *E* isomer is observed with a rate constant $k_{Z\rightarrow E} = 2.5 \times 10^{-6} \text{ s}^{-1}$ at 293 K.

In the case of **Si-Z-Azo** the thermal back isomerization to **Si-E-Azo** is significantly different (Figure 4a): the plot is not linear and the rate of the thermal isomerization is much faster than that of the model compound. For example, if we prepare two samples of **Z-Azo** and **Si-Z-Azo** in toluene with the same concentration of azobenzene chromophore ($5.0 \times 10^{-5} \text{ M}$), after 10 minutes, the conversion of the model compound is 4% and that of the azobenzene functionalized SiNCs is 68%. As previously reported in literature,^{36–38} azobenzene thermal isomerization is strongly dependent not only on the nature of the substituents (identical in our case), but also on the polarity of the solvent. The rate is enhanced in polar aprotic solvents due to stabilization of the dipolar transition state.³⁷ Indeed, the thermal isomerization of **Z-Azo** and **Si-Z-Azo** is much faster in chloroform, a more polar solvent compared to toluene (Figure S11).

Therefore, we ascribe the observed differences to the fact that in **Si-Z-Azo** the *Z*-azobenzene chromophores experience a more polar environment compared to the toluene solution because of the presence of 15 *Z*-azobenzene chromophores within a nanoscale object. During the thermal isomerization, polar *Z*-isomers are converted to less polar *E*-isomers, so that the polarity experienced by azobenzene chromophores changes over time and this makes the observed plot deviating from the usual linearity.

This is an unprecedented result: most of the literature reports on nanoparticles or dendrimers functionalized with multiple photoswitching azobenzene units^{22,39} describe a first-order rate constant for the *Z*→*E* thermal isomerization, unless *E*→*Z* photoswitching is completely inhibited by strong π - π stacking in very compact layers. We believe that the deviation from the first order kinetics is observed in our case because of the huge number of azobenzene covalently linked to a small nanoparticle (diameter of ca. 3 nm): this creates a new environment experienced by the azobenzene units.

Quenching and sensitization processes. It is important to consider possible quenching and sensitization processes between azobenzene chromophores and the silicon core in the hybrid system. First of all, we can rule out sensitization of the

silicon emission upon excitation of azobenzene chromophores. Indeed, the excitation spectrum of **Si-E-Azo** performed at $\lambda_{\text{em}} = 730 \text{ nm}$ well matches the absorption profile of the reference sample **Si-But** (Figure S7), demonstrating that azobenzene excitation does not sensitize the silicon core emission, as expected by the very short lifetime of the lowest singlet excited states characteristic of the azobenzene chromophores.³⁵ The same holds true in the case of **Si-Z-Azo**.

As reported in Table 1, the emission quantum yields and lifetimes of **Si-E-Azo** and **Si-Z-Azo** upon selective excitation of the silicon core is significantly lower than that of the reference sample **Si-But**. This result demonstrates that the azobenzene chromophore quenches the Si core emission. This quenching process can be related to energy or electron transfer mechanisms.

Photoinduced electron transfer is not a plausible mechanism based on a previous study published by some of us²⁹ since efficient quenching is observed only for species easier to be reduced compared to *E* and *Z*-isomers of azobenzene (reduction potential of azobenzene derivatives is in the range -1.3 / -1.4 V vs SCE).^{40–42}

As far as energy transfer is concerned, selective excitation of the silicon core of **Si-Z-Azo** at 660 nm results in the sensitized *Z*→*E* isomerization (Figure 4b): starting from two identical solutions of **Si-Z-Azo** in toluene thermostated at 261 K a faster conversion is observed upon 660 nm irradiation (green circles) compared to the sample kept in the dark (blue circles). This result is ascribed to a photosensitization of the *Z*→*E* photoisomerization via selective population of the lowest triplet excited state of *Z*-azobenzene. On the other hand, no significant photosensitized isomerization is observed for the **Si-E-Azo** upon selective excitation of the silicon core.

A similar selective *Z*→*E* photosensitization has been previously reported for molecular dyads⁴⁰ and multichromophoric dendrimers.^{39,43,44}

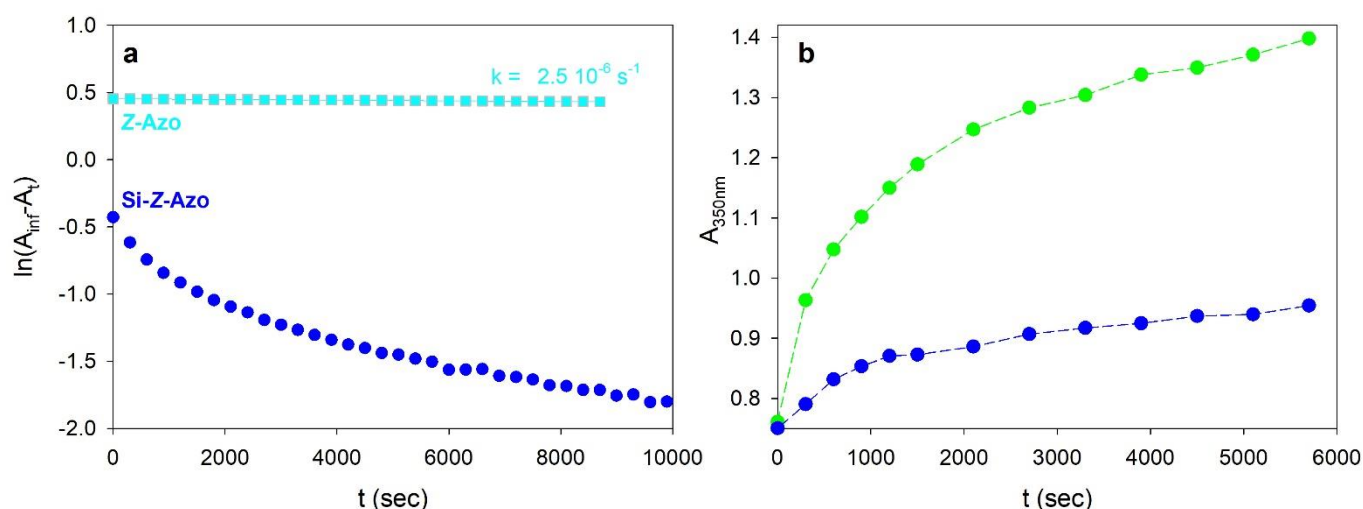


Figure 4. (a) Thermal isomerisation of **Z-Azo** ($5.0 \times 10^{-5} \text{ M}$, cyan squares) and **Si-Z-Azo** ($2.5 \times 10^{-6} \text{ M}$, blue circles) in toluene solution at 293 K. (b) Thermal (blue circles) vs photosensitized (green circles, $\lambda_{\text{irr}} = 660 \text{ nm}$) isomerization of **Si-Z-Azo** in toluene at 261 K.

As previously observed, energy transfer is expected to take place in both **Si-E-Azo** and **Si-Z-Azo**, but, because of the shape of the azobenzene excited state potential energy curve, it leads to excited state geometries that can only deactivate to the trans isomer, leading to a selective $Z \rightarrow E$ photosensitized isomerization. The theoretical interpretation of the direct and sensitized photoisomerization of azobenzene has been the object of much debate.^{45–47} A description of the phenomenon is even more difficult in our hybrid system since the silicon core can affect the isomerization process by electronic perturbation as well as by steric constraints.

Conclusions

Semiconducting silicon nanocrystals functionalized with azobenzene chromophores were synthesized by a 3-step procedure, resulting in silicon nanocrystals with diameter of ca. 3 nm appended with 15 azobenzene units, as an average.

The interplay between the photoswitchable azobenzene and the luminescent properties of the inorganic nanocrystals was investigated.

The reversible and fatigue-resistant photoswitching behaviour of azobenzene chromophores is preserved with $E \rightarrow Z$ and $Z \rightarrow E$ photoisomerization quantum yield similar to the model compound. Upon excitation at 365 nm, almost quantitative $E \rightarrow Z$ photoisomerization takes place and a strong change in polarity of the resulting hybrid system is observed: the partition ratio of **Si-E-Azo** between cyclohexane and methanol is 65:35, while that of **Si-Z-Azo** is <20:80.

The interaction between the organic and inorganic part is clearly visible in the decreased luminescence intensity of the nanocrystals upon selective excitation of the silicon core. This result has been ascribed to a photoinduced energy transfer to the appended azobenzene chromophores, which results in a

$Z \rightarrow E$ photoisomerization, as previously observed in the case of molecular dyads and dendrimers.

The most striking difference between the azobenzene model compound and the hybrid system is the kinetic of the thermal $Z \rightarrow E$ isomerization: the hybrid system exhibits a much faster kinetic and a deviation from the first-order kinetic. This behaviour is rationalized based on the change in environment polarity experienced by azobenzene chromophores at the surface of nanocrystals: from a polar environment created by *Z*-isomers, at the beginning, to a less polar environment as soon as the isomerisation proceeds. This behaviour is unprecedented and it is likely related to the large number of azobenzene confined in a small nano-object (average diameter of the silicon core ca. 3 nm).

Future studies are aimed at the functionalization of SiNCs with other photoswitching molecules and increasing the photomodulation of the luminescent properties of the nanocrystals according to the isomerization state of the appended photoswitch.

Conflicts of interest

There are no conflicts to declare.

Acknowledgements

The University of Bologna is gratefully acknowledged for financial support.

Notes and references

- § When the nucleophilic substitution is not complete and chlorosilane groups are still present at the surface of the

nanocrystals, we observe nanocrystal precipitation within few hours. The colloidal stability of the sample is thus an experimental evidence of the success of step (iii).

- 1 C. M. Gonzalez, M. Iqbal, M. Dasog, D. G. Piercec, R. Lockwood, T. M. Klapötke, J. G. C. Veinot, T. M. Klapotke and J. G. C. Veinot, *Nanoscale*, 2014, **6**, 2608–2612.
- 2 M. Dasog, J. Kehrle, B. Rieger and J. G. C. Veinot, *Angew. Chemie - Int. Ed.*, 2016, **55**, 2322–2339.
- 3 R. Mazzaro, F. Romano and P. Ceroni, *Phys. Chem. Chem. Phys.*, 2017, **19**, 26507–26526.
- 4 *Faraday Discuss.*, 2020, **222**, 1–438.
- 5 H. Kim, M. Seo, M.-H. Park and J. Cho, *Angew. Chem. Int. Ed.*, 2010, **49**, 2146–2149.
- 6 S. Bhattacharjee, I. M. C. M. Rietjens, M. P. Singh, T. M. Atkins, T. K. Purkait, Z. Xu, S. Regli, A. Shukaliak, R. J. Clark, B. S. Mitchell, G. M. Alink, A. T. M. Marcelis, M. J. Fink, J. G. C. Veinot, S. M. Kauzlarich and H. Zuilhof, *Nanoscale*, 2013, **5**, 4870–4883.
- 7 J. M. Buriak, *Chem. Mater.*, 2014, **26**, 763–772.
- 8 J. A. Kelly, E. J. Henderson and J. G. C. Veinot, *Chem. Commun.*, 2010, **46**, 8704–8718.
- 9 C. E. Rowland, D. C. Hannah, A. Demortière, J. Yang, R. E. Cook, V. B. Prakapenka, U. Kortshagen and R. D. Schaller, *ACS Nano*, 2014, **8**, 9219–9223.
- 10 L. Ravotto, Q. Chen, Y. Ma, S. A. Vinogradov, M. Locritani, G. Bergamini, F. Negri, Y. Yu, B. A. Korgel and P. Ceroni, *Chem*, 2017, **2**, 550–560.
- 11 X. Wen, P. Zhang, T. A. Smith, R. J. Anthony, U. R. Kortshagen, P. Yu, Y. Feng, S. Shrestha, G. Coniber and S. Huang, *Sci. Rep.*, 2015, **5**, 12469.
- 12 R. Mazzaro, M. Locritani, J. K. Molloy, M. Montalti, Y. Yu, B. A. Korgel, G. Bergamini, V. Morandi and P. Ceroni, *Chem. Mater.*, 2015, **27**, 4390–4397.
- 13 M. Locritani, Y. Yu, G. Bergamini, M. Baroncini, J. K. J. K. Molloy, B. A. B. A. Korgel and P. Ceroni, *J. Phys. Chem. Lett.*, 2014, **5**, 3325–3329.
- 14 H. M. D. Bandara and S. C. Burdette, *Chem. Soc. Rev.*, 2012, **41**, 1809–1825.
- 15 A. A. Beharry and G. A. Woolley, *Chem. Soc. Rev.*, 2011, **40**, 4422–4437.
- 16 M. Villa, G. Bergamini, P. Ceroni and M. Baroncini, *Chem. Commun.*, 2019, **55**, 11860–11863.
- 17 Z. Zhang, S. Zhang, J. Zhang, L. Zhu and D. Qu, *Tetrahedron*, 2017, **73**, 4891–4895.
- 18 E. Chevallier, C. Monteux, F. Lequeux and C. Tribet, *Langmuir*, 2012, **28**, 2308–2312.
- 19 Y. Zhao, *Macromolecules*, 2012, **45**, 3647–3657.
- 20 P. Ahonen, D. J. Schiffrin, J. Paprotny and K. Kontturi, *Phys. Chem. Chem. Phys.*, 2007, **9**, 651–658.
- 21 G. L. Hallett-Tapley, C. D’alfonso, N. L. Pacioni, C. D. McTiernan, M. González-Béjar, O. Lanzalunga, E. I. Alarcon and J. C. Scaiano, *Chem. Commun.*, 2013, **49**, 10073–10075.
- 22 R. Klajn, J. F. Stoddart and B. A. Grzybowski, *Chem. Soc. Rev.*, 2010, **39**, 2203–2237.
- 23 S. Bonacchi, A. Cantelli, G. Battistelli, G. Guidetti, M. Calvaresi, J. Manzi, L. Gabrielli, F. Ramadori, A. Gambarin, F. Mancin and M. Montalti, *Angew. Chemie Int. Ed.*, 2016, **55**, 11064–11068.
- 24 S. Saeed, J. Yin, M. A. Khalid, P. A. Channar, G. Shabir, A. Saeed, M. Arif Nadeem, C. Soci and A. Iqbal, *J. Photochem. Photobiol. A Chem.*, 2019, **375**, 48–53.
- 25 H. Javed, K. Fatima, Z. Akhter, M. A. Nadeem, M. Siddiq and A. Iqbal, *Proc. R. Soc. A Math. Phys. Eng. Sci.*, 2016, **472**, 20150692.
- 26 C. M. Hessel, E. J. Henderson and J. G. C. Veinot, *Chem. Mater.*, 2006, **18**, 6139–6146.
- 27 M. R. Hessel, C. M.; Reid, D.; Panthani, M. G.; Rasch, B. A. Goodfellow, B. W.; Wei, J.; Fujii, H.; Akhavan, V.; Korgel, C. M. Hessel, D. Reid, M. G. Panthani, M. R. Rasch, B. W. Goodfellow, J. Wei, H. Fujii, V. Akhavan and B. A. Korgel, *Chem. Mater.*, 2012, **24**, 393–401.
- 28 I. M. D. Hohlein, J. Kehrle, J. G. C. Veinot, B. Rieger, I. M. D. Höhle, J. Kehrle, T. K. Purkait, J. G. C. Veinot and B. Rieger, *Nanoscale*, 2015, **7**, 914–918.
- 29 A. Arrigo, R. Mazzaro, F. Romano, G. Bergamini and P. Ceroni, *Chem. Mater.*, 2016, **28**, 6664–6671.
- 30 Y. Liu, C. Yu, H. Jin, B. Jiang, X. Zhu, Y. Zhou, Z. Lu and D. Yan, *J. Am. Chem. Soc.*, 2013, **135**, 4765–4770.
- 31 R. J. Clark, M. Aghajamali, C. M. Gonzalez, L. Hadidi, M. A. Islam, M. Javadi, M. H. Mobarok, T. K. Purkait, C. J. T. Robidillo, R. Sinelnikov, A. N. Thiessen, J. Washington, H. Yu and J. G. C. Veinot, *Chem. Mater.*, 2017, **29**, 80–89.
- 32 R. Mazzaro, A. Gradone, S. Angeloni, G. Morselli, P. G. Cozzi, F. Romano, A. Vomiero and P. Ceroni, *ACS Photonics*, 2019, **6**, 2303–2311.
- 33 D. Beri, M. Jakoby, I. A. Howard, D. Busko, B. S. Richards and A. Turshatov, *Dalt. Trans.*, 2020, **49**, 2290–2299.
- 34 Y. Yu, G. Fan, A. Fermi, R. Mazzaro, V. Morandi, P. Ceroni, D.-M. Smilgies and B. A. Korgel, *J. Phys. Chem. C*, 2017, **121**, 23240–23248.
- 35 M. Quick, A. L. Dobryakov, M. Gerecke, C. Richter, F. Berndt, I. N. Ioffe, A. A. Granovsky, R. Mahrwald, N. P. Ernsting and S. A. Kovalenko, *J. Phys. Chem. B*, 2014, **118**, 8756–8771.
- 36 F. Serra and E. M. Terentjev, *Macromolecules*, 2008, **41**, 981–986.
- 37 K. S. Schanze, T. F. Mattox and D. G. Whitten, *J. Org. Chem.*, 1983, **48**, 2808–2813.
- 38 P. D. Wildes, J. G. Pacifici, G. Irick, D. G. Whitten, P. D. Wildes, J. G. Pacifici, G. Irick, D. G. Whitten, P. D. Wildes, J. G. Pacifici and G. Irick, *J. Am. Chem. Soc.*, 1971, **93**, 2004–2008.
- 39 F. Vögtle, M. Gorka, R. Hesse, P. Ceroni, M. Maestri and V. Balzani, *Photochem. Photobiol. Sci.*, 2002, **1**, 45–51.
- 40 P. Ceroni, I. Laghi, M. Maestri, V. Balzani, S. Gestermann, M. Gorka and F. Vögtle, *New J. Chem.*, 2002, **26**, 66–75.
- 41 G. Grampp, C. Mureşanu and S. Landgraf, *J. Electroanal. Chem.*, 2005, **582**, 171–178.
- 42 G. Klopman and N. Doddapaneni, *J. Phys. Chem.*, 1974, **78**, 1825–1828.
- 43 A. Archut, G. C. Azzellini, V. Balzani, L. De Cola and F. Vögtle, *J. Am. Chem. Soc.*, 1998, **120**, 12187–12191.
- 44 F. Puntoriero, P. Ceroni, V. Balzani, G. Bergamini and F.

- Vögtle, *J. Am. Chem. Soc.*, 2007, **129**, 10714–10719.
- 45 P. Bortolus and S. Monti, *J. Phys. Chem.*, 1979, **83**, 648–652.
- 46 S. Monti, G. Orlandi and P. Palmieri, *Chem. Phys.*, 1982, **71**, 87–99.
- 47 E. Fischer, *J. Am. Chem. Soc.*, 1968, **90**, 796–797.